Development of a high gradient rf system using a nanocrystalline soft magnetic alloy

Chihiro Ohmori,* Eizi Ezura, Keigo Hara, Katsushi Hasegawa, Yasuhiro Makida, Ryotaro Muto, Masahiro Nomura, Toru Ogitsu, Taihei Shimada, Alexander Schnase,† Koji Takata, Akira Takagi, Fumihiko Tamura, Kazuhiro Tanaka, Makoto Toda, Masanobu Yamamoto, and Masahito Yoshii

J-PARC Center, KEK and JAEA, 2-4 Shirakata-Shirane, Tokai, Naka, Ibaraki, Japan 319-1195

(Received 3 October 2013; published 18 November 2013)

The future high intensity upgrade project of the J-PARC (Japan Proton Accelerator Research Complex) MR (Main Ring) includes developments of high gradient rf cavities and magnet power supplies for high repetition rate. The scenario describing the cavity replacements is reported. By the replacement plan, the total acceleration voltage will be almost doubled, while the number of rf stations remains the same. The key issue is the development of a high gradient rf system using high impedance magnetic alloy, FT3L. The FT3L is produced by the transverse magnetic field annealing although the present cavity for the J-PARC adopts the magnetic alloy, FT3M, which is annealed without magnetic field. After the test production using a large spectrometer magnet in 2011, a dedicated production system for the FT3L cores was assembled in 2012. This setup demonstrated that we can produce material with 2 times higher μ_p'Qf product compared to the cores used for present cavities. In this summer, the production system was moved to the company from J-PARC and is used for mass production of 280 FT3L cores for the J-PARC MR. The cores produced in the first test production are already used for standard machine operation. The operation experience shows that the power loss in the cores was reduced significantly as expected.

DOI: 10.1103/PhysRevSTAB.16.112002 PACS numbers: 29.20.dk

I. INTRODUCTION

The Japan Proton Accelerator Research Complex (J-PARC) aims to deliver 1 MW beam from Rapid Cycling Synchrotron (RCS) to Materials and Life Science Experimental Facility (MLF), 750 kW beam from the Main Ring (MR) to the Neutrino Experimental Facility, and 100 kW to the Hadron Experimental Facility [1]. Both the RCS and MR adopt magnetic alloy (MA) loaded cavities for beam acceleration [2,3]. The MA loaded cavity system provides two advantages to handle a high intensity beam:

(a) A higher field gradient can be obtained because the characteristics of the material is more stable at a high rf field than ferrite materials as shown in Fig. 1. This difference exists, because the saturation field of the material, B_s of 1.8 T [4,5], is much higher than that of ferrite. This is a very important point to design the J-PARC RCS to be a compact machine.

(b) A simple rf system without a tuning loop is suitable to handle a high intensity beam. Because the MA loaded system has a wide and variable bandwidth, the frequency variation for proton acceleration can be handled without a tuning circuit, which is necessary for a ferrite loaded system[6].

Figure 1 shows the characteristics of different magnetic materials for the accelerator use. The vertical axis is the μ_p'Qf product which is given by the shunt impedance of a magnetic core, R_p. It shows that the characteristics of the magnetic alloy is stable in a high rf magnetic field, B_{RF}, that is, in a high rf voltage. The μ_p'Qf product is given by

$$R_p = \mu_0(\mu_p'\mathrm{Qf})t\ln\frac{\mathrm{O.D.}}{\mathrm{I.D.}}, \tag{1}$$

where O.D., I.D., and t are the outer diameter, inner diameter, and the thickness of a toroidal core. The suffix p means "parallel" to express the magnetic materials are treated as a parallel circuit. The complex relative permeability is

$$\mu_r = \mu_s' - j\mu_s'', \tag{2}$$

$$\mu_r^{-1} = \mu_p'^{-1} + j\mu_p''^{-1}. \tag{3}$$

The Q value of the material is given by

$$Q = \mu_s'/\mu_s'' = \mu_p''/\mu_p'. \tag{4}$$

The product μ_p'Qf is independent of the size and shape of the magnetic core and is used to evaluate magnetic materials.

Although the magnetic alloy loaded cavities are used for both the RCS [7] and MR [8], some details are different. As the RCS needs a wide bandwidth for acceleration from low energy (181 MeV), and it also needs a dual harmonic rf

*chihiro.ohmori@kek.jp
†Present address: GSI, Darmstadt, Germany.

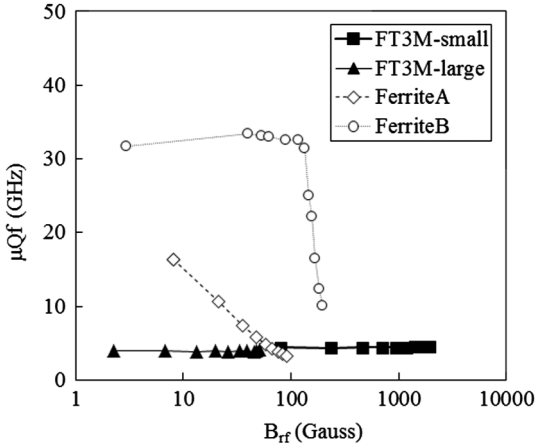

FIG. 1. Magnetic flux density dependence of magnetic materials. The vertical axis is the product of μ'_pQf (relative parallel permeability, Q value, and frequency), which is proportional to the shunt impedance. Ferrite A is a typical low-Q ferrite core with 500 mm O.D. where the magnetic flux density dependence was observed. Ferrite B is a high-Q type; however, it also shows the so-called high loss effects. FT3M-small and FT3M-large denotes MA cores of 570 mm O. D. and 70 mm O.D., respectively. These MA cores show a constant shunt impedance up to 2 kGauss.

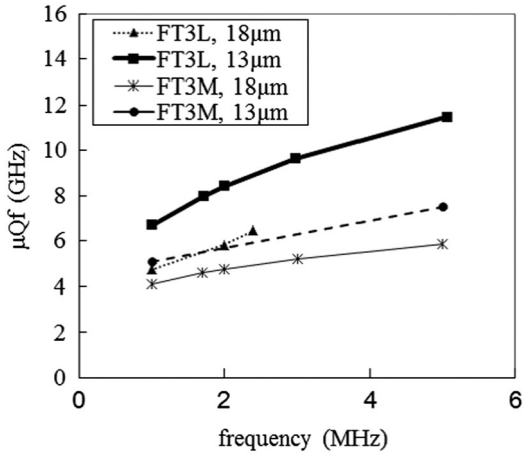

FIG. 2. Characteristics of MA cores. The present FT3M core (solid line) with 18 μm layer thickness can be improved by the FT3L with 13 μm thickness (bold line). The dashed and dotted lines mean the products of the FT3M with 13 μm thickness and the FT3L with 18 μm thickness, respectively. Both dashed and dotted lines show about 20% improvement compared to the present FT3M.

[9–11], the Q value of the RCS cavity is about 2, defined by an external inductor [12]. In the MR, the frequency variation is only 3% and a higher Q value is preferred because of the heavy beam loading. Thus a cut core configuration is used to control the Q value [2,13–15].

The RCS has demonstrated the ability to accelerate a half MW beam [16,17] and routinely delivered a 300 kW beam to the MLF. The RCS cavities operate as dual harmonic rf systems, which is necessary to reduce the space charge effect during injection. The system realized by a single $Q = 2$ cavity is also helpful to save the space in a compact synchrotron.

The MR routinely delivered a 230 kW beam for neutrino experiments in 2013. For further improvement, we plan to increase the cycling rate of the MR from the present 0.4 Hz to about 1 Hz[18,19]. A project to improve the magnet power supplies for high repetition has been started. In parallel, the upgrade program of the J-PARC rf cavity is started. The key issue is, as usual, the improvement of the material to be loaded into the cavities. The magnetic alloy, FT3L [20], which has 2 times better characteristics than the present magnetic alloy, FT3M, is used.

The magnetic alloy, which the J-PARC is using, is a soft-magnetic nanocrystalline material [4,5]. It is known that the magnetic property of MA can be changed by applying an external magnetic field during annealing [21]. The external transverse field causes a tilt of the magnetic hysteresis loop. The magnetic alloy, which is annealed in the transverse magnetic field, is called FT3L. Magnetic alloy annealed without the magnetic field is called FT3M and, so far, the FT3M is used for the rf cavities. And, it is also known that the characteristics depend on the thickness of the ribbon, which is used to wind the ring shaped core. To avoid a large eddy current loss between ribbons, an SiO2 coating is created on one side of the thin ribbons for the electrical insulation [22]. Figure 2 shows the difference of material and ribbon-thickness dependence. The vertical axis is the product of μ'_pQf (relative parallel permeability, Q value, and frequency), which is proportional to the shunt impedance.

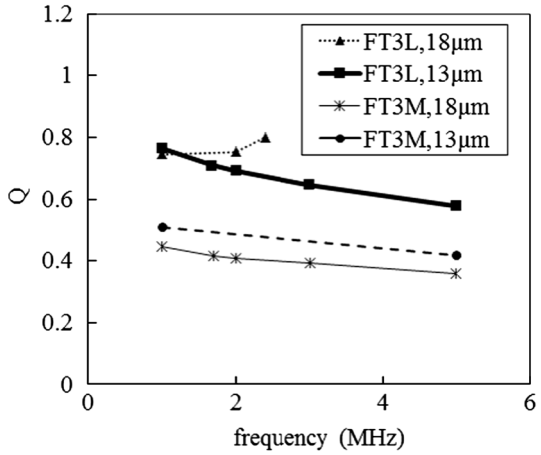

FIG. 3. Q value of MA cores. The present FT3M core (solid line) with 18 μm layer thickness can be improved by the FT3L with 13 μm thickness (bold line). The dashed line means the Q value of the FT3M with 13 μm thickness and shows higher value than 18 μm one. The dotted line is that of the FT3L with 18 μm thickness and shows about the same Q value as the 13 μm one.

Figure 2 clearly shows that the $\mu'_p Qf$ product becomes 2 times larger when the external magnetic field was applied during annealing on the MA core using 13 μm thick ribbon. Figure 3 indicates the Q value of these two materials. It shows that the $\mu'_p Qf$ improvement is mainly caused by increasing the Q value.

II. THE PROOF OF PRINCIPLE TEST OF LARGE FT3L CORE

Although the FT3L seems to have better characteristics than the FT3M, no production system existed to make a large FT3L core for accelerator use. The first proof of principle experiments to produce large FT3L cores were performed in 2011 (see Fig. 4). The 300-ton magnet was originally used for a frequency modulated cyclotron and it had been modified as a spectrometer magnet for a nuclear experiment. Fortunately, there was about 1 year and we were allowed to use this magnet for the FT3L production tests. The FM magnet is 5.395 m(H) $\times$ 3.67 m(V) $\times$ 2.12 m(L). The gap height is 0.9 m and the diameter of the pole piece is 1.7 m. Because of the large pole piece compared to our magnetic alloy core, the magnetic field was expected to be almost uniform.

The oven was designed to anneal 850 mm diameter ring cores for the J-PARC. The size of the oven is 1.4 m(H) $\times$ 0.64 m(V) $\times$ 1.7 m(L). And, the inner size is 1.1 m(H) $\times$ 0.37 m(V) $\times$ 1.4 m(L). The uniformity of the temperature is $\pm 2.9\,^{\circ}$C in the area where the core is located. This is a quite good uniformity for such a large size oven. However, this means that the heat inside the oven does not escape easily. Therefore, we apply forced cooling using a higher nitrogen gas flow for the cool down process. The first FT3L core which was made by this system is shown in Fig. 5. The magnetic field of a few kilo Gauss was applied during annealing. All FT3L cores which were produced showed good characteristics as expected [20].

FIG. 4. The proof of principle system using a spectrometer magnet. An annealing oven is located between the magnet poles. A load lifter was used to set a core in the oven.

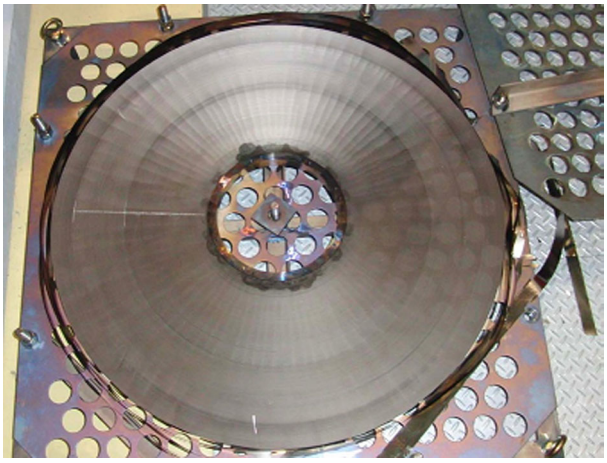

FIG. 5. The large size FT3L core annealed by the proof of principle system.

III. TEST OF FT3L CAVITY

The first FT3L large cores for accelerator use were manufactured, according to the recipe that is used for the FT3M cores. There was no significant difficulty to process the FT3L cores. The FT3L core is coated for use in the water tank. The core was cut as shown in Fig. 6 and the cut surface was treated by a diamond polishing. After protecting the polished surface, the core is assembled and installed in a water tank as shown in Fig. 7. Six FT3L cores were installed in a MR rf cavity in summer 2012, as shown in Fig. 8.

The first FT3L cavity cell impedance is 1300 Ω and this is 20% higher than other FT3M cavities using a ribbon of 18 μm thickness. As the thickness of the FT3L cores was 25 mm, which is 10 mm thinner than standard FT3M cores that are used in other tanks, we put a 30 mm thick spacer disc to fit the FT3L cores into the water tanks, which were designed for the thicker FT3M cores. The cavity has been working properly. Figure 9 shows the power consumption in a half cell of cavity calculated by the temperature rise of the cavity cooling water. It shows the power loss in the

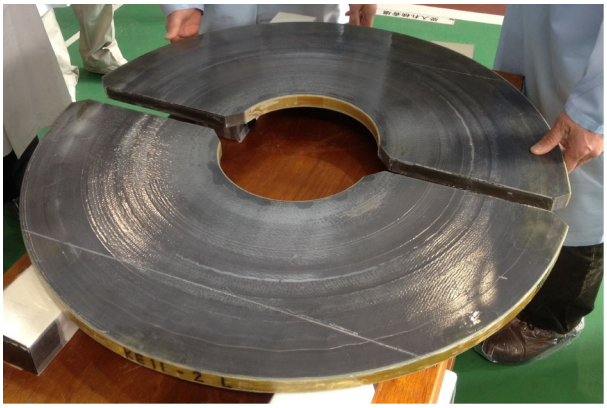

FIG. 6. The FT3L cut core before diamond polishing.

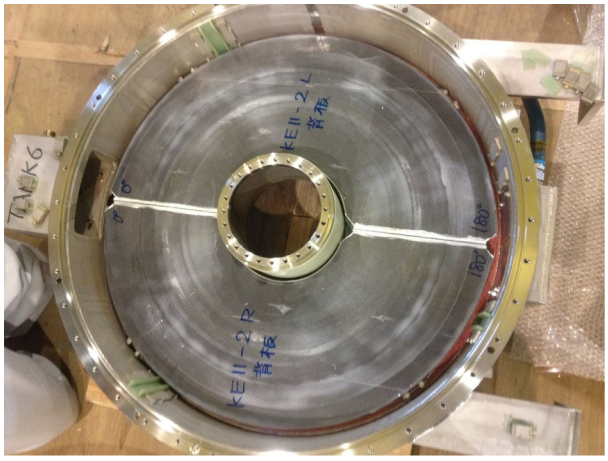

FIG. 7. The FT3L cut core is installed in a water tank.

cavity is much less than that in other existing FT3M cavities as expected.

The variation of cavity impedance over time is shown in Fig. 10. The cavities consist of three cavity cells. The impedance of the cavity no. 1 is given as a parallel circuit of one FT3L cell and two standard FT3M cells. The other

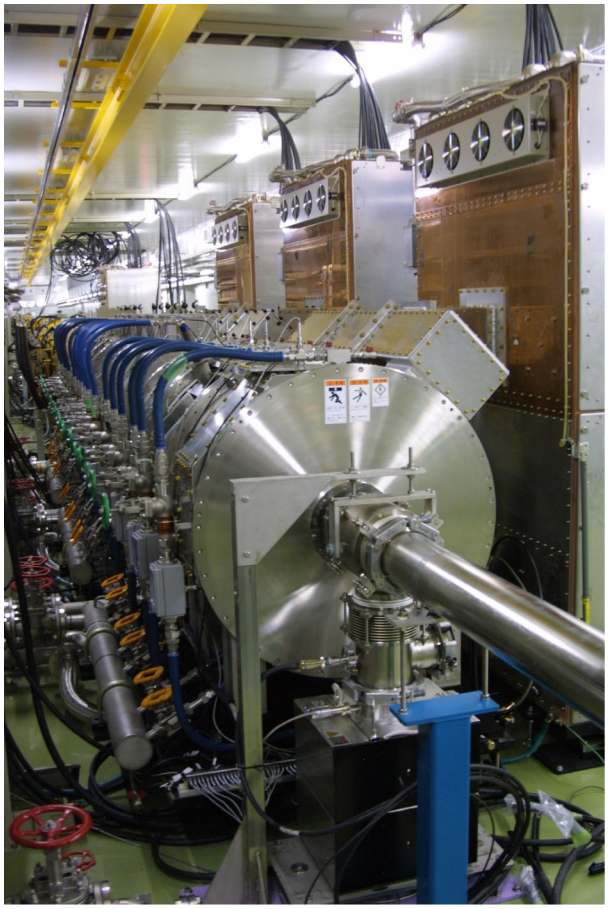

FIG. 8. The FT3L cores are installed in one cell of a 3-cell cavity in the J-PARC MR.

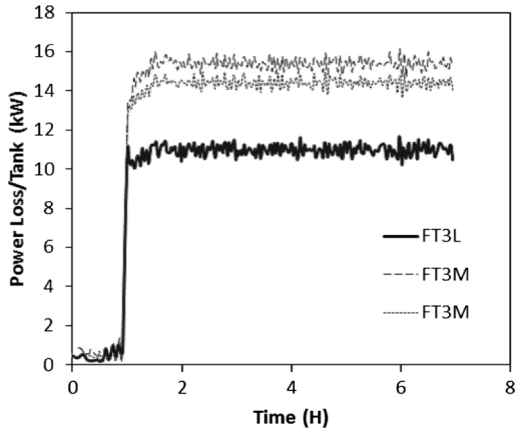

FIG. 9. Power consumption in a half cavity cell calculated by temperature rise of cooling water during machine operation. The gap voltage was 11.7 kV during the measurements. Because of the higher impedance compared to the other cavities, the temperature rise of the FT3L cavity cell (bold line) is much lower than that of the other FT3M cavity cells (dashed and dotted lines). The temperature and flow rate has 5%–7% and 5% errors, respectively. The power consumption in the FT3L cell is consistent with the cavity impedance measurements.

cavities consist of three FT3M cells. Because the latest production of the FT3M cores that have 5%–7% higher impedance than the typical FT3M cores were installed in cavity no. 1, the whole cavity impedance is higher than expected. This figure shows the impedance of three cavities that were active in January 2013. During four months, the cavity impedance of the FT3L cavity is as stable as the other FT3M cavities.

The power consumption in a water tank of the FT3L cell was about 10 kW and this is consistent with the expected power loss from the voltage pattern. These results show clearly the advantage of a high impedance cavity. The heat

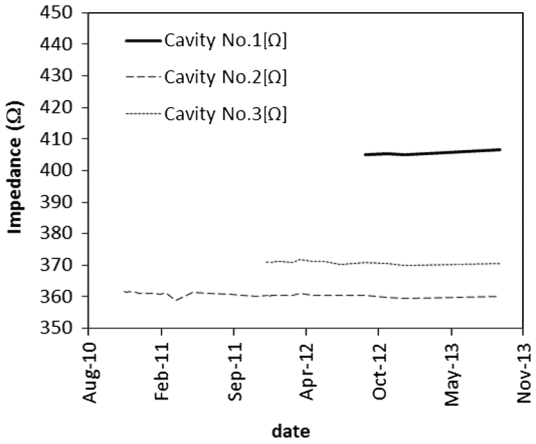

FIG. 10. Variation of the cavity impedance during machine operation. The cavity no. 1 (bold line), which has one cell using the FT3L core, has a higher impedance than the other cavities (dashed and dotted lines). It has been operated for a few months and the cavity impedance is as stable as the others.

FIG. 11. The FT3L core production system using the Kappa magnet. The inner size of the oven is 1.1 m(W) × 0.37 m(H) × 1.4 m(L) to anneal the large size core up to 0.85 m diameter.

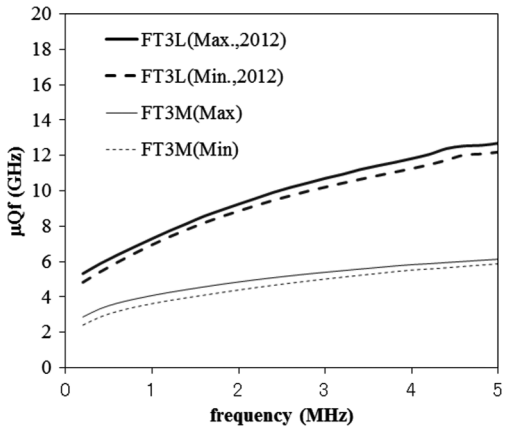

FIG. 12. Characteristics of MA cores for the J-PARC accelerator use. The FT3M cores (thin lines) are currently used for the J-PARC. The recent production (bold lines) shows 2 times higher performance.

load on the magnetic cores is reduced and this will reduce the risks of overheating caused by high rf power. The high power operation of the FT3L loaded cavity shows promising results for the future production of the FT3L cavities.

IV. A NEW MASS PRODUCTION SYSTEM FOR FT3L CORES

The large FM magnet [20] that was used for the first test production of the FT3L cores was returned for a nuclear physics experiment in the J-PARC Hadron Facility. A new setup for long term use was assembled using the "Kappa" magnet in the J-PARC [23]. Figure 11 shows the Kappa magnet and the annealing oven. The Kappa magnet was modified to fit the large oven. Because the distance between the oven and magnet pole pieces becomes close, the speed to cool the annealed core becomes faster compared to the test production. It helps to anneal the cores in a limited time with controlled oven temperature.

The production of the FT3L cores was started in December 2012 and the results are shown in Fig. 12. The μ'_pQf product of the FT3L cores is 2 times higher than that of the FT3M cores that we are currently using in the J-PARC. Comparing with the FT3L core in Fig. 2 which has a small size, the μ'_pQf product of the FT3L cores is equivalent. This means the mass production system works properly.

V. MASS PRODUCTION OF FT3L CAVITIES

A. Cavity design

For the upgrade of the MR, the present FT3M cavities will be replaced by new FT3L cavities to increase the rf voltage. Our strategy is as follows:

(a) Without modifying the anode power supply, auxiliary power supplies and final stage amplifier, the necessary voltage can be achieved.
(b) Some cavities and amplifiers can be moved in the same straight section. All power supplies, cavities, and amplifiers should be located in the same building and same straight section.

As shown in Fig. 12, the μ'_pQf product of the FT3L cores becomes 2 times higher than that of the present FT3M cores. This factor-of-2 improvement can be used to design a compact cavity putting less material in a cavity and/or to design a high impedance cavity.

We chose a compromise to design upgrade cavities for the J-PARC. The factor-of-2 improvement is used to reduce the materials by 40% and to increase the cavity impedance by 40%. The length of cavity cells can be reduced from the present 590 mm to 505 mm. And, the number of cells that can be driven by the present amplifier can be increased from the present 3 to 5.

Figure 13 shows the upgrade scenario of the cavities. Seven cavities will be replaced by new 5-cell cavities and two by 4-cell ones. The total rf voltage will be 560 kV while the minimum rf voltage for 1 Hz operation is 440 kV. The rf voltage of 560 kV corresponds to the acceleration of a 10 eVs emittance beam with the filling factor of 70% after the controlled emittance blowup. The voltage of 440 kV is obtained by the simulation to accelerate the 1 MW-equivalent RCS beam without the emittance blowup. The margin is necessary to obtain the large rf bucket to handle the high intensity beam without beam loss and to increase the system reliability. It also shows all cavities and amplifiers can be kept in the same straight section. The upgrade of the J-PARC MR will be done without a large modification of the building and power supplies on the ground. Although the total cavity impedance seen by the beam will be increased by a factor of 2,

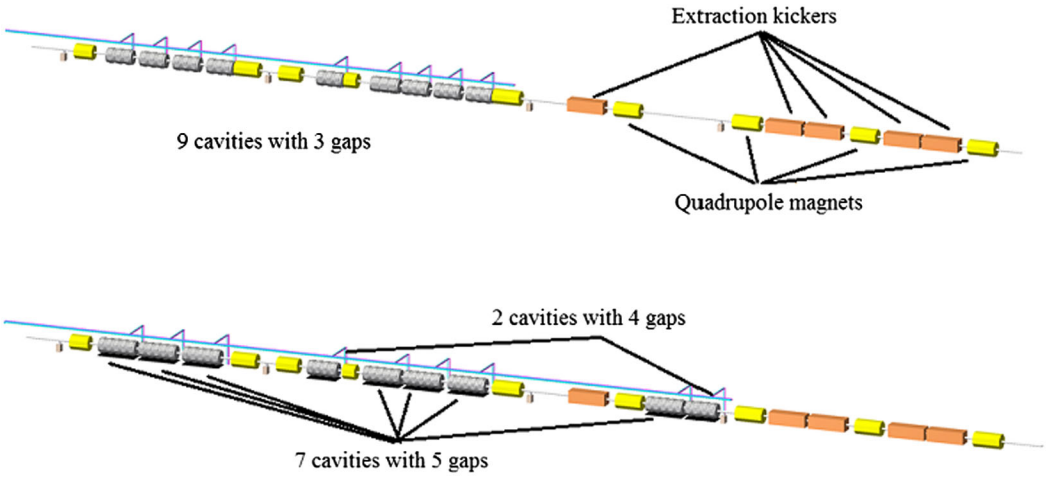

FIG. 13. Upgrade scenario of the J-PARC MR cavities. The present cavities (upper) will be replaced by the FT3L cavities (lower) in 2014–2016. The total rf voltage will become 560 kV providing enough margin as the required rf voltage for 1 Hz operation is 440 kV according to a simulation.

the present beam loading compensation is expected to manage this.

B. Mass production

The mass production system of the FT3L cores was disassembled to move to the company. The production was started in this summer for new FT3L cavities. The mass production of the FT3L cores for the MR will continue until 2016.

After this, we will consider starting the production of the FT3L cores for the MR second harmonic cavities. The FT3L technique will be applied for the RCS systems to increase the beam power, too.

VI. MECHANISM

A. Magnetic field annealing

Magnetic field annealing is the powerful tool used to control the hysteresis of the magnetic alloys [24,25]. A flat type hysteresis loop can be obtained by transverse field annealing. In contrast, a high remanence ratio material, which has a rectangular shaped hysteresis loop, can be obtained by longitudinal field annealing.

During the transverse field annealing, a uniaxial anisotropy is induced perpendicular to the ribbon axis. Then, an easy axis of magnetization, which is determined by the crystal axis, is formed parallel to the transverse field and perpendicular to the ribbon axis. The magnetic domain wall is also formed perpendicular to the ribbon axis. The FT3L is produced by the transverse annealing.

During the longitudinal field annealing, a uniaxial anisotropy is parallel to the ribbon axis. An easy axis is formed parallel to the ribbon axis. The domain wall is formed parallel to the ribbon axis. Another material, FT3H, is produced by the longitudinal annealing.

The round loop results after conventional annealing without a magnetic field. A random distribution of uniaxial anisotropies is induced parallel to the magnetization vector in each domain. The FT3M is produced by this scheme.

B. Core loss

The rf power loss in the magnetic core (P_c) consists of the eddy current loss (P_e) and hysteresis one (P_h), in case of a magnetic alloy core,

$$P_c = P_h + P_e. \tag{5}$$

The eddy current loss can be written as

$$P_e = P_e^{\mathrm{cla}} + P_e^{\mathrm{ex}}, \tag{6}$$

where P_e^{ex} means the excessive eddy current loss that depends on the magnetic field annealing. It was called anormalous eddy current loss [24]. P_e^{cla} means the classical eddy current loss and is given by [25]

$$P_e^{\mathrm{cla}} = \frac{3}{x}\frac{\sinh x - \sin x}{\cosh x - \cos x}\frac{\pi^2 d^2 B_m^2 f^2}{6\rho}, \tag{7}$$

$$\approx \frac{\pi^2 d^2 B_m^2 f^2}{6\rho}, \quad \text{if } x \ll 1, \tag{8}$$

with $x = 2\sqrt{f/f_{\mathrm{W}}}$, where

$$f_{\mathrm{W}} = \frac{4\rho}{\pi\mu_0\mu_{\mathrm{i}}d^2} \tag{9}$$

is the limiting frequency above which the rf magnetic field no longer fully penetrates. In the equation, d, B_m, and ρ are thickness, rf magnetic field, and resistivity, respectively. f_{W} is about 2.6 MHz for 13 μm thick ribbon and about 2 MHz for 18 μm one, respectively. The difference of f_{W}

is not big because the FT3L with 13 μm thickness has higher permeability, μ_s, than that with the 18 μm one.

The domain wall displacement is regarded as the main cause of the excessive eddy current loss. When the domain wall is parallel to the magnetic field during usage, a displacement occurs. The motion of the wall causes the loss. The other loss is caused by the magnetization rotation, which is the motion of the magnetization in the domain. The magnetization rotation is a fast process and causes a much smaller loss than the domain wall displacement.

In the case of the FT3H core, the rf magnetic field is parallel to the ribbon axis, that is, domain wall. When the direction of the magnetic field is changed, the domain wall displacement occurs. Because the domain wall displacement is a slow process, the excessive loss is large and the μ'_pQf product is much lower than others as shown in Fig. 14 [24].

The magnetization process of the FT3M during rf operation is a mixture of magnetization rotation and domain wall displacement. When the thickness of the ribbon is reduced, the domain wall displacement still exists and the μ'_pQf product cannot be improved much as shown in Fig. 2.

In case of the FT3L core, we expect P_e^{ex} becomes much smaller than that of the FT3H because the domain wall displacement rarely occurs [24]. The normal eddy current loss and magnetization rotation are the cause of the loss in the FT3L. Because the domain wall motion is rare, the FT3L has higher μ'_pQf product than other magnetic alloys. And, the 13 μm thick ribbon improved the μ'_pQf product of the FT3L by 50% as is shown in Fig. 2. The use of a thinner ribbon in the case of the FT3M can give an improvement of 20%.

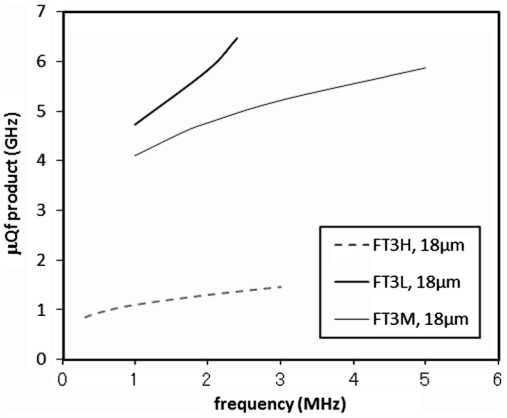

FIG. 14. Characteristics of the magnetic alloy core, FT3M, FT3L, and FT3H with same ribbon thickness of 18 μm. The FT3M cores (thin lines) are currently used for the J-PARC. The FT3L (bold lines) shows about 20% higher μ'_pQf product than the FT3M. The FT3H is the material annealed with the magnetic field with a different direction than that of the FT3L. This material shows a lower impedance than the other materials. The behavior of the FT3H explains the loss mechanism in the magnetic alloy core.

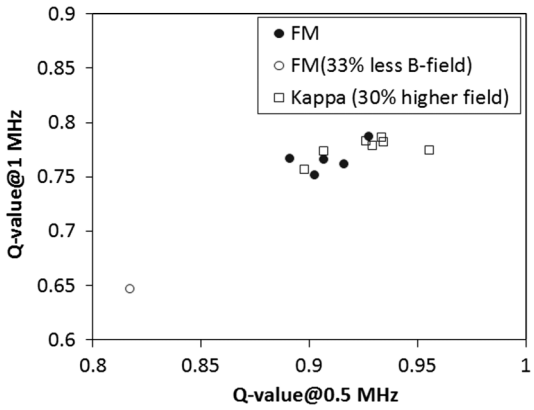

FIG. 15. Scatter plot of Q value of the FT3L cores at 0.5 MHz and 1 MHz. The black circle and open box mean the typical productions using the FM and Kappa magnet, respectively. The difference on the Q values between two different production systems is clearly shown. The open circle is the case when a FT3L core is annealed in the low field. The low magnetic field annealing causes the reduction of the Q value.

C. Discussions

The latest production using the Kappa magnet shows higher impedance than the production using the large FM magnet [23]. There are two major improvements to produce the FT3L cores. One is the improvement of the packing factor, that is, the density of the magnetic material in a core. The other is the improvement of the magnetic field because of a different magnet. Figure 15 shows a scatter plot of the Q values at 0.5 and 1 MHz. As shown in Figs. 2 and 3, the increase of the Q value causes the increase of the μ'_pQf product. Because the maximum field in the Kappa magnet is 30% higher than that of the FM magnet, the Q value of the FT3L cores becomes larger. However, the difference is much smaller than the difference between the typical production by the FM magnet and that with 33% less field. It suggests that the magnetic field for the FT3L mass production is almost high enough.

Although Fig. 15 shows the tendency of the magnetic field dependence on the Q value of the FT3L cores, it is still unknown how much improvement on the μ'_pQf product is caused by the magnetic field, the packing factor, and others. There are several key technologies to improve the core performance, that is, magnetic field, quality of ribbon, temperature control, and the control of the stress force. These technologies will be improved during the mass production of the FT3L cores for J-PARC MR.

VII. CONCLUSIONS

This paper reports the recent progress of a magnetic alloy cavity using a material, FT3L. An MR cavity, where one cell was loaded with the FT3L cores, has been in stable machine operation for half a year. A new mass production

system of the FT3L cores for accelerator use worked very well. The mass production system was moved to a company for the production of the FT3L cavities. All J-PARC MR cavities will be replaced with the FT3L cavities for the J-PARC upgrade.

ACKNOWLEDGMENTS

The authors would like to thank the J-PARC accelerator team and the KEK accelerator laboratory for supporting this work to improve the cavity performance. We would like to express our gratitude to Professors Y. Kimura, K. Oide, T. Koseki, F. Naito, Y. Yamazaki, H. Kobayashi, K. Hasegawa, M. Kinsho, S. Anami, Y. Kobayashi, M. Ieiri, Y. Fujii, Y. Miyake, K. Nishiyama, K. Shimomura, A. Koda, Mr. O. Araoka, and H. Ohata for their advice and encouragement. We are deeply grateful to Professor Y. Mori for his leadership in developing the magnetic alloy cavity in the early stage. We would like to mention that the discussion with Professor Y. Iwashita, Drs. F. Pedersen, R. Garoby, and M. Paoluzzi in the early stage of the cavity development was highly supportive. We also want to thank Mr. Yoshizawa and K. Ogura from Hitachi Metal Co. for fruitful discussions on the finemet materials.

[1] Accelerator technical design report for J-PARC, Report No. JAERI- TECH 2003-044, 2003.
[2] C. Ohmori *et al.*, in *Proceedings of the 18th Particle Accelerator Conference, New York, 1999* (IEEE, New York, 1999), pp. 413–417.
[3] C. Fougeron *et al.*, in *Proceedings of the 2nd European Particle Accelerator Conference, Nice, France, 1990* (Editions Frontieres, Gif-sur-Yvette Cedex, France, 1990), pp. 961–963.
[4] Nanocrystalline soft magnetic material, finemet, http://www.hitachi-metals.co.jp/e/products/elec/tel/pdf/hl-fm9-e.pdf.
[5] Y. Yoshizawa, J. Appl. Phys. **64**, 6044 (1988).
[6] I. S. Gardner, in *RF Engineering for Particle Accelerators, Proceedings of the CERN Accelerator School* (CERN, Geneva, 1993), pp. 349–374.
[7] M. Yamamoto *et al.*, in *Proceedings of the 22nd Particle Accelerator Conference, Albuquerque, New Mexico* (IEEE, New York, 2007), pp. 1532–1534.
[8] M. Yoshii *et al.*, in *Proceedings of the 22nd Particle Accelerator Conference, Albuquerque, New Mexico* (IEEE, New York, 2007), pp. 1511–1513.
[9] C. Ohmori, M. Kanazawa, K. Noda, M. Kawashima, T. Misu, Y. Mori, A Sugiura, A. Takagi, and T. Uesugi, Nucl. Instrum. Methods Phys. Res., Sect. A **547**, 249 (2005).
[10] F. Tamura *et al.*, Phys. Rev. ST Accel. Beams **12**, 041001 (2009).
[11] M. Yamamoto *et al.*, Nucl. Instrum. Methods Phys. Res., Sect. A **621**, 15 (2010).
[12] A. Schnase *et al.*, in *Proceedings of the 22nd Particle Accelerator Conference, Albuquerque, New Mexico* (IEEE, New York, 2007), pp. 2131–2133.
[13] M. Yoshii *et al.*, in *Proceedings of the 7th European Particle Accelerator Conference, Vienna, Austria, 2000* [Joint Accelerator Conferences Website (JACoW), CERN, Geneva, 2000], pp. 984–986.
[14] M. Nomura *et al.*, in *Proceedings of the 2nd International Particle Accelerator Conference, San Sebastián, Spain* (EPS-AG, Spain, 2011), pp. 107–109.
[15] M. Yoshii *et al.*, in *Proceedings of the 3rd International Particle Accelerator Conference, New Orleans, Louisiana, 2012* (IEEE, Piscataway, NJ, 2012), pp. 3211–3213.
[16] H. Hotchi *et al.*, Phys. Rev. ST Accel. Beams **12**, 040402 (2009).
[17] H. Hotchi *et al.*, in *Proceedings of the 1st International Particle Accelerator Conference (IPAC 13)* [Joint Accelerator Conferences Website (JACoW), CERN, Geneva, 2013], pp. 3836–3838.
[18] Y. Sato *et al.*, in *Proceedings of the 2nd International Particle Accelerator Conference, San Sebastián, Spain* (EPS-AG, Spain, 2011), pp. 598–600.
[19] T. Koseki *et al.*, Prog. Theor. Exp. Phys. **02**, 004 (2012).
[20] C. Ohmori *et al.*, in *Proceedings of the 2nd International Particle Accelerator Conference, San Sebastián, Spain* (EPS-AG, Spain, 2011), pp. 2885–2887.
[21] Y. Tanabe *et al.*, in *Proceedings of 1998 Asian Particle Accelerator Conference (APAC 98)* [Joint Accelerator Conferences Website (JACoW), CERN, Geneva, 1998], pp. 390–392.
[22] M. Nomura *et al.*, Nucl. Instrum. Methods Phys. Res., Sect. A **668**, 83 (2012).
[23] C. Ohmori *et al.*, in *Proceedings of the forth International Particle Accelerator Conference (IPAC 13)* [(Joint Accelerator Conferences Website (JACoW), CERN, Geneva, 2013], pp. 1152–1154.
[24] Y. Yoshizawa, IEEE Trans. Magnetics, **25**, 3324 (1989).
[25] G. Herzer, in *Handbook of Magnetic Materials*, edited by K. Buschow (Elsevier Science, North Holland, 1997), Vol. 10, chap. 3, pp. 415–462.